SUPPLEMENTARY INFORMATION

Novel Ternary AgIICoIIIF5 Fluoride: Synthesis, Structure and Magnetic Characteristics

Daniel Jezierski[1]*, Zoran Mazej[2]*, Wojciech Grochala[1]*

Contents

SI.I Overview of the $A^{II}B^{III}F_5$ fluoride family

	Compound	Mangetic GS*	T_t [K]	REF	STRUCTURE
TM-TM	$CrTiF_5$	Fi	26	[1]	*C*2/*c* (Cr_2F_5- type)
	$CrVF_5$	Fi	40	[1]	*C*2/*c* (Cr_2F_5- type)
	$MnCrF_5$	AF	6	[2]	*C*2/*c*
	$CdMnF_5$	n.d.	n.d.	[3]	*C*2/*c*
AE-TM	$CaFeF_5$	AF	21	[4]	$P2_1/c$
	$CaCrF_5$	P	---	[5]	*C*2/*c*
	$CaTiF_5$	P	---	[6]	*I*2/*c*
	$CaMnF_5$	n.d.	n.d.	[3]	*C*2/*c*
	$BaFeF_5$	AF	35	[7]	*I*4
	$BaTiF_5$	n.d.	n.d.	[6]	*I*4/*m*
	$BaVF_5$	AF	20	[8]	*I*4
	$SrVF_5$	AF	2	[4]	$P2_1/c$
	$SrCrF_5$	P	---	[8]	*I*4
	$SrFeF_5$	n.d.	n.d.	[9]	$P2_1/c$
PT-TM	$CrAlF_5$	P	---	[1]	*C*2/*c* (Cr_2F_5- type)
	$MnAlF_5$	P	---	[10]	ORTORHOMBIC
AE-PT	alpha-$CaAlF_5$	---	---	[5]	*C*2/*c*
	beta-$CaAlF_5$	---	---	[11]	$P2_1/c$
	$SrAlF_5$	---	---	[7]	*I*4
	$PbTF_5$ (T = Al, Ga)	---	---	[12]	n. d.
	$BaInF_5$	---	---	[13]	n. d.
OTHER	$Mn(Al,Fe)F_5$	Fi	18-34	[10]	ORT

* Fi – ferrimagnetic, AF – antiferromagnetic, P – paramagnetic; n.d. stands for not determined

SI.II Structural data for $AgCoF_5$

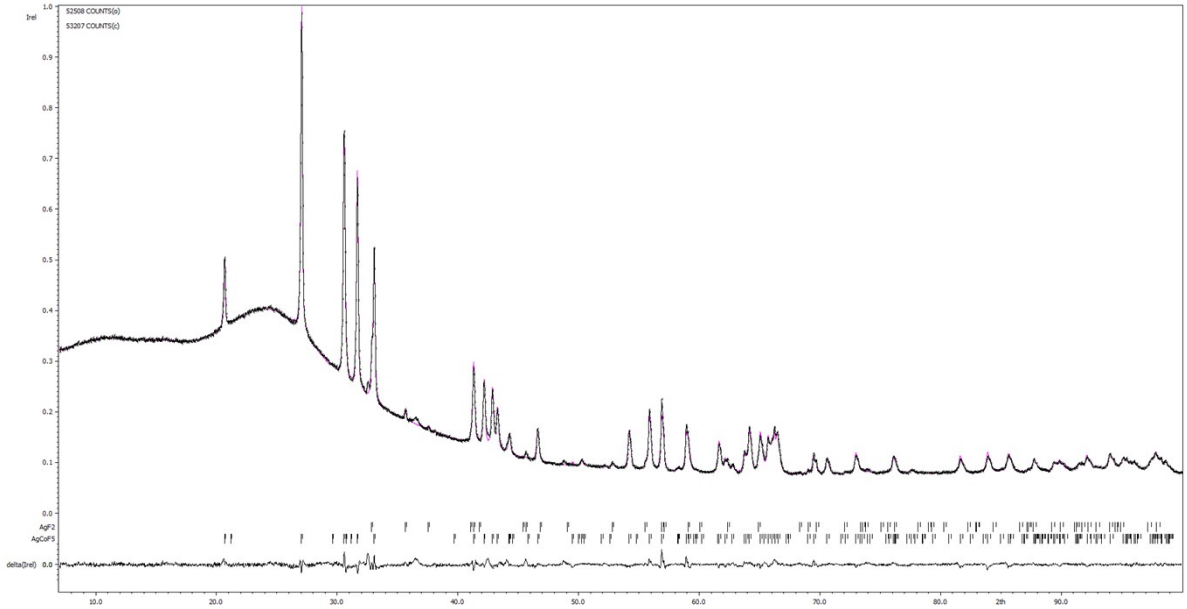

Figure SI1. Rietveld refinement of the X-ray pattern for the powder from the first synthetic approach. GoF = 1.15, Rp = 0.98, wRp = 1.36

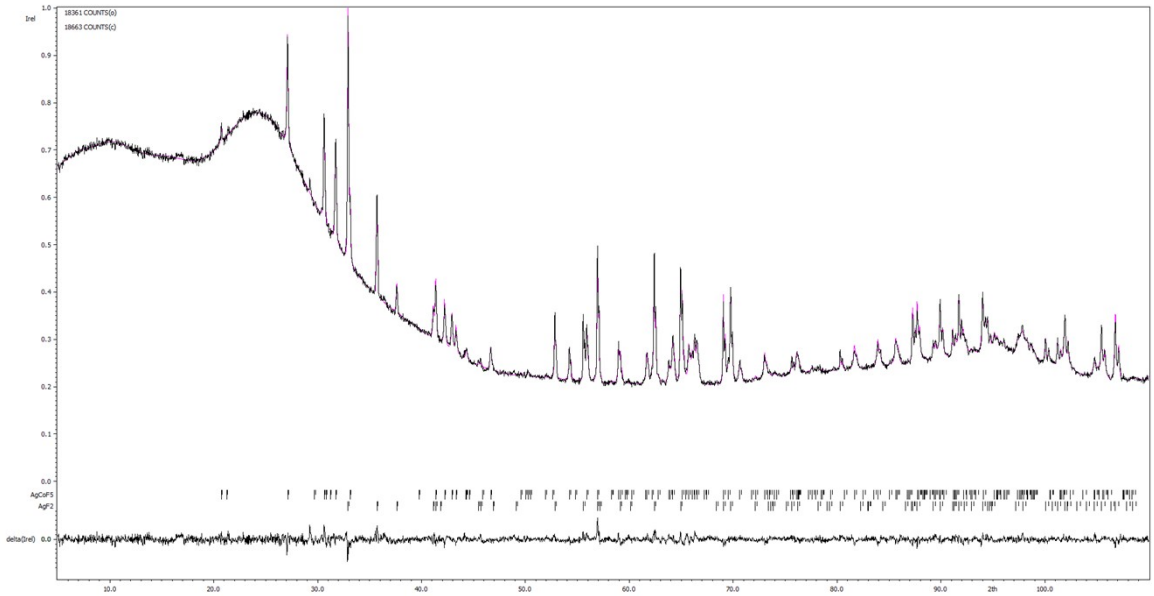

Figure SI2. Rietveld refinement of the X-ray pattern for the powder from the second synthetic approach. GoF = 1.66, Rp = 1.12, wRp = 1.68.

Table SI1. Unit cell parameters of AgF_2 and $AgCoF_5$ obtained from Rietveld refinement of two samples 1 (**S1**) and sample 2 (**S2**).

S	Phase	Parameters					Molar ratio	Uncertainty [%]	Fitting parameters		
		a [Å]	b [Å]	c [Å]	V [Å³]	β [°]			GoF	Rp	wRp
1	AgF_2	5.546	5.831	5.091	164.636	90	0.04	3	1.66	1.12	1.68
	$AgCoF_5$	7.274	7.628	7.529	375.552	115.98	0.96	4			
2	AgF_2	5.550	5.836	5.095	165.026	90	0.44	8	1.15	0.98	1.36
	$AgCoF_5$	7.280	7.635	7.536	376.507	115.98	0.56	7			

Table SI2. Structural details of $AgCoF_5$ with atomic positions.

Space group	***C2/c* (15)**	*Temperature*	**298K**	*Radiation*	**Co Kα**
Unit cell [Å]	*a* = 7.274414 (2), *b* = 7.627744(2), *c* = 7.529471 (2)			α = γ = 90°	β =115.976(4)°
Atom	**x**	**y**	**z**	**U_{iso} [Å^2]**	**Occupancy**
Co	0.000	0.000	0.000	0.003 (14)	1
Ag	0.000	0.500	0.000	0.010 (13)	1
F1	0.000	-0.038 (5)	0.250	0.019 (18)	1
F2	0.793 (18)	0.513 (6)	0.624 (18)	0.007 (15)	1
F3	-0.028 (3)	0.235 (2)	0.448 (3)	0.013 (15)	1

It is important to note that the exact determination the positions of the fluorine atoms is a major challenge, even when analyzing single-crystal samples. The structural data of $AgCoF_5$ were determined using the powder X-ray diffraction technique on polycrystalline samples. This approach was supported by incorporating computational methods at various stages of the structure determination process. It is therefore essential to bear in mind that the positional data of the light atoms may exhibit subtle degrees of approximation.

Table SI3. Structural parameters of $AgCoF_5$ from experimental and various theoretical methods.

Methods	**a [Å]**	**b [Å]**	**c [Å]**	**V [Å^3]**	**β [°]**
Rietveld	7.274 (2)	7.628(2)	7.529(2)	375.580(19)	115.976(4)
DFT+U (U = 5 eV)	7.187	7.643	7.535	375.305	114.948
DFT+U (U = 8 eV)	7.157	7.607	7.508	370.475	115.003
SCAN	7.269	7.749	7.586	382.619	116.431
HSE06	7.201	7.661	7.527	376.855	114.819

Table SI4. Bond lengths and angles in the $AgCoF_5$ structure: Rietveld and theoretical methods. These theoretical calculations are based on idealized conditions (p,T → 0), which leads to some inherent discrepancies compared to experimental data obtained under ambient conditions.

Methods	**dM-M [Å]**	**dM-F [001] [Å]**	**dM-F (001) [Å]**	**Bond angle [°]**
Rietveld	Co-Ag: 3.637(10), 3.814(10) Ag-Ag and Co-Co: 3.765(10)	Ag-F: 2.562(12) Co-F: 1.905(6)	Ag-F: 2.090(16), 2.052(16) Co-F: 1.827(16), 1.921(13)	Co-F-Co: 162.0(3)° [001]; Ag-F-Ag: 107.6(5)° [001] Co-F-Ag: 158.9(12)° [010]; 130.1(8)° [100];
DFT+U (U = 5 eV)	Co-Ag: 3.593, 3.822 Ag-Ag and Co-Co: 3.768	Ag-F: 2.587 Co-F: 1.916	Ag-F: 2.071, 2.056 Co-F: 1.816, 1.943	Co-F-Co: 158.9° [001]; Ag-F-Ag: 107.9° [001] Co-F-Ag: 158.9° [010]; 127.9° [100];
DFT+U (U = 8 eV)	Co-Ag: 3.579, 3.803 Ag-Ag and Co-Co: 3.754	Ag-F: 2.571 Co-F: 1.911	Ag-F: 2.053, 2.043 Co-F: 1.817, 1.943	Co-F-Co: 158.9° [001]; Ag-F-Ag: 108.4° [001] Co-F-Ag: 158.6° [010]; 127.7° [100];
SCAN	Co-Ag: 3.635, 3.874 Ag-Ag and Co-Co: 3.793	Ag-F: 2.563 Co-F: 1.919	Ag-F: 2.081, 2.085 Co-F: 1.826, 1.926	Co-F-Co: 162.4° [001]; Ag-F-Ag: 109.1° [001] Co-F-Ag: 164.1° [010]; 130.1° [100];
HSE06	Co-Ag: 3.600, 3.831 Ag-Ag and Co-Co: 3.763	Ag-F: 2.608 Co-F: 1.910	Ag-F: 2.070, 2.059 Co-F: 1.822, 1.928	Co-F-Co: 160.2° [001]; Ag-F-Ag: 106.9° [001] Co-F-Ag: 159.6° [010]; 129.1° [100];

SI.III Comparison of Rietveld fits for *C*2/*c* and *C*2/*m* space groups

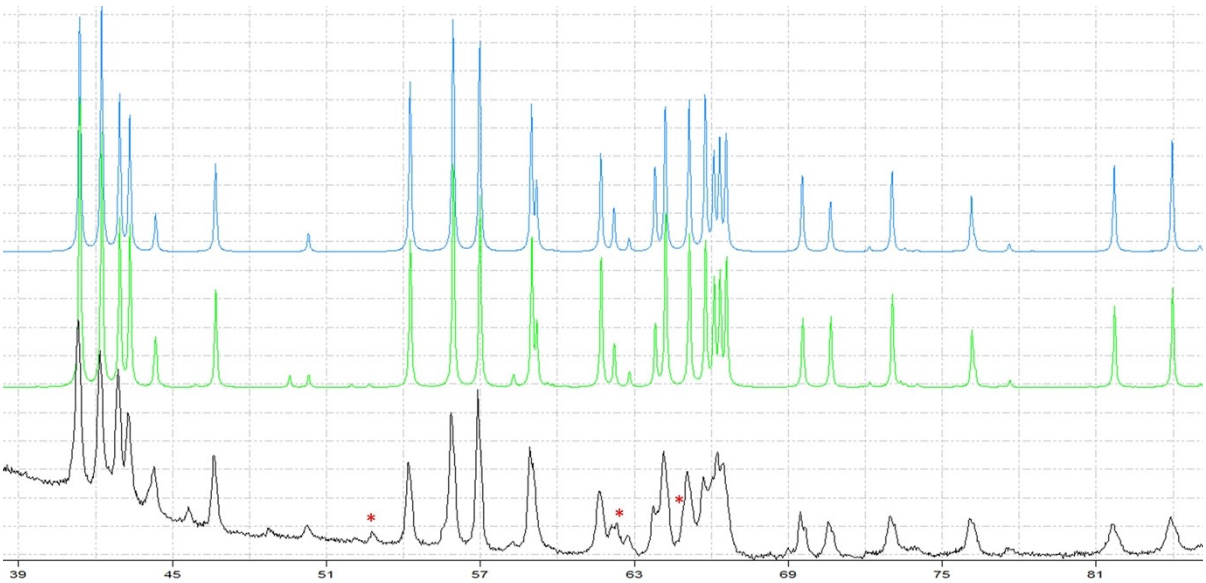

Figure SI3. Comparison between experimental diffractogram of **S1** (black line), model diffractogram for $AgCoF_5$ structure in *C*2/*c* (green line) and *C*2/*m* structure (blue line). Asterisks indicate the positions of potential reflexes originating from AgF_2 impurities (or may constitute shoulder of the one from $AgCoF_5$).

Table SI5. Structure and fitting parameters of $AgCoF_5$ from the very first cycle of Rietveld refinement process of C2/c and C2/m structures, based on experimental diffractogram from **S1**.

$AgCoF_5$	**Parameters**					**Fitting parameters**		
group space	**a [Å]**	**b [Å]**	**c [Å]**	**V [Å³]**	**β [°]**	**GoF**	**Rp**	**wRp**
*C*2/*c* (Z = 4)	7.276	7.629	7.531	375.803	115.981	2.56	1.63	2.59
*C*2/*m* (Z = 2)	7.276	7.629	3.765	187.886	115.981	2.91	1.88	2.95

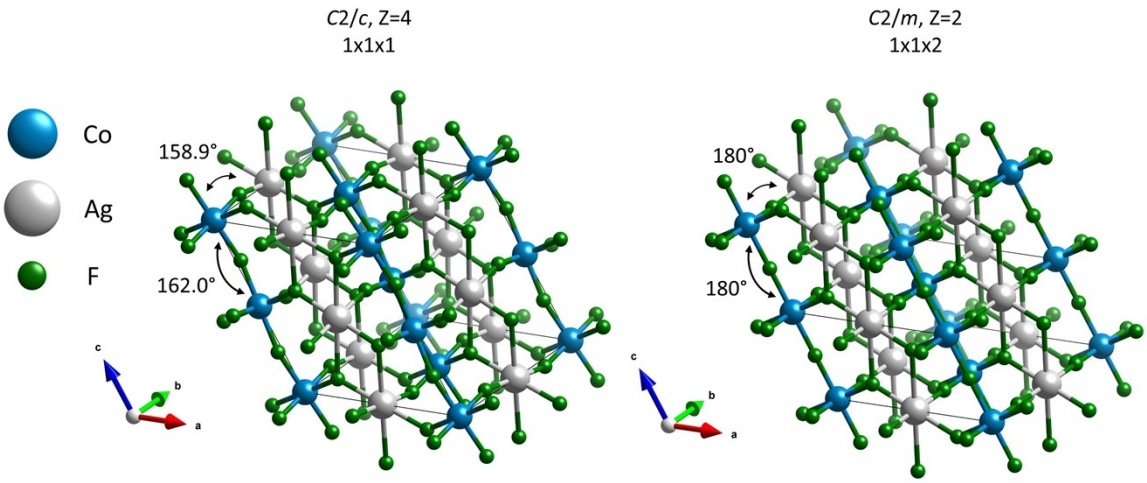

Figure SI4. $AgCoF_5$ in C2/c (left) and C2/m (right, 1x1x2 supercell) space group. The unit cell is drawn as a solid line.

SI.IV Experimental and theoretical phonon frequencies of $AgCoF_5$

Table SI6. Phonon vibration frequencies and their symmetries from DFT+U computations and band positions identified in IR and Raman spectra for $AgCoF_5$. Darkened columns indicate bands that are not observable due to symmetry constraints (forbidden by selection rules). Band intensities are categorized as follows: vs - very strong, s - strong, m - medium, w - weak, vw - very weak, sh - shoulder. "Silent" in shaded columns refers to non-active bands. "---" indicates the absence of the corresponding band in the experimental spectra. The indication "n.d." refers to band positions outside the spectroscopes' measurement range. Positions in cm^{-1}.

#	DFT+U	Symmetry	IR	RAMAN	#	DFT+U	Symmetry	IR	RAMAN
1	570	B_g		591vs	22	219	A_u	*silent*	
2	555	A_u	*silent*		23	215	B_u	218m	
3	551	B_u	548sh		24	215	A_u	*silent*	
4	534	A_g		---	25	193	A_u	*silent*	
5	519	B_u	510vs		26	182	B_u	177m	
6	471	B_g		491m	27	178	A_u	*silent*	
7	469	A_u	*silent*		28	176	B_g		173sh
8	452	B_u	452vs		29	165	B_u	---	
9	393	A_u	*silent*		30	156	A_u	*silent*	
10	391	A_g		393sh	31	139	B_u	141vw	
11	376	B_g		367sh	32	110	A_g		114vs
12	352	B_u	356s		33	102	B_g		100sh
13	348	A_u	*silent*		34	98	A_u	*silent*	
14	314	A_u	*silent*		35	95	B_u	92w	
15	303	B_u	---		36	79	A_g		n.d.
16	284	B_g		282sh	37	64	A_u	*silent*	
17	274	A_g		273sh	38	56	B_u	n.d.	
18	266	A_g		259m	39	45	B_g		n.d.
19	245	B_u	253m		40	-1	B_u		
20	242	B_g		241sh	41	-1	A_u		
21	220	A_g		223vw	42	-2	B_u		

Table SI7 Combination vibrations and overtones observed in the spectra in Figure 5. Positions in cm^{-1}.

IR [cm^{-1}]	RAMAN [cm^{-1}]	ASSIGNEMENT
110		111 B_u -> 45 + 56 (IR_{Bu}+R_{Bg})
272		291 (B_u) -> 177 + 114 (IR_{Bu} + R_{Ag})
630		624 (B_u) -> 510 + 114 (IR_{Bu} + R_{Ag})
	802	808 (A_g) -> 452 + 356 (IR_{Bu}+IR_{Bu})
	1074	1082 (A_g) -> 591 + 491 (R_{Bg} + R_{Bg})
	1229	Overtone ($2 \cdot B_g = 2 \cdot 591$ cm^{-1})

SI.V Magnetic data

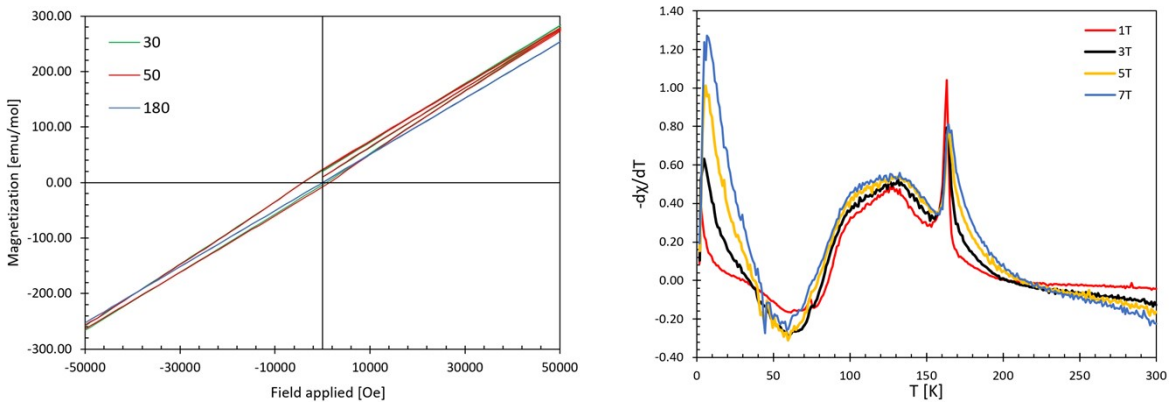

Figure SI5. Magnetization curves at 30 K, 50 K, 180 K for **S1** as a function of the applied field (left) and first derivatives of the sample magnetization (-dχ/dT) as a function of T dependence on the left, measured at different fields.

AgF_2 (from Ag_3F_8 decomposition) DJ24

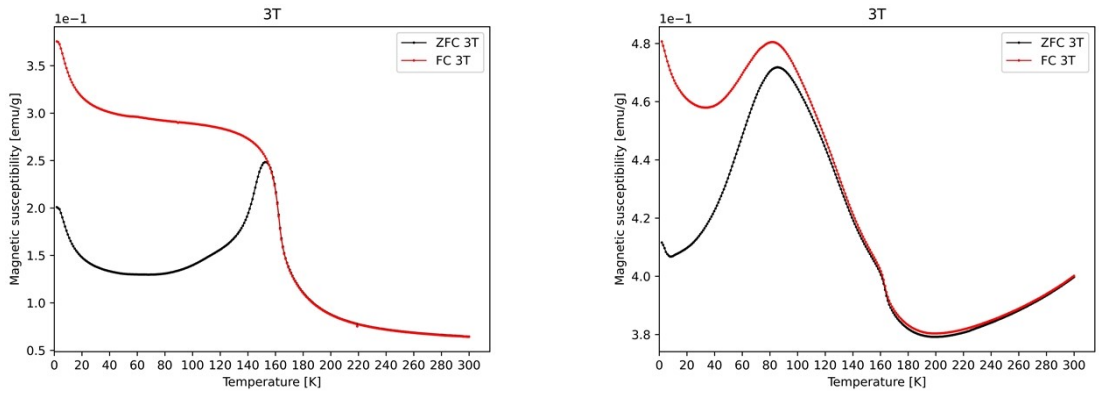

Figure SI6. Magnetization for AgF_2 (left) and S1 (right) – mainly $AgCoF_5$ with AgF_2 traces at 30 kOe vs temperature [K].

A simple subtraction of the contribution of AgF_2 to the overall magnetic response of the sample does not eliminate the feature at 163 K (see **Figure SI6**), which is characteristic of the magnetic transition in silver(II) difluoride, from the susceptibility plot. This leads to considerable complications when analyzing the measurement results and makes it impossible to fit a magnetic model. In addition, there are many other complications, including: 1) different magnetic spins for magnetic ions; 2) low-dimensionality of magnetic interactions.

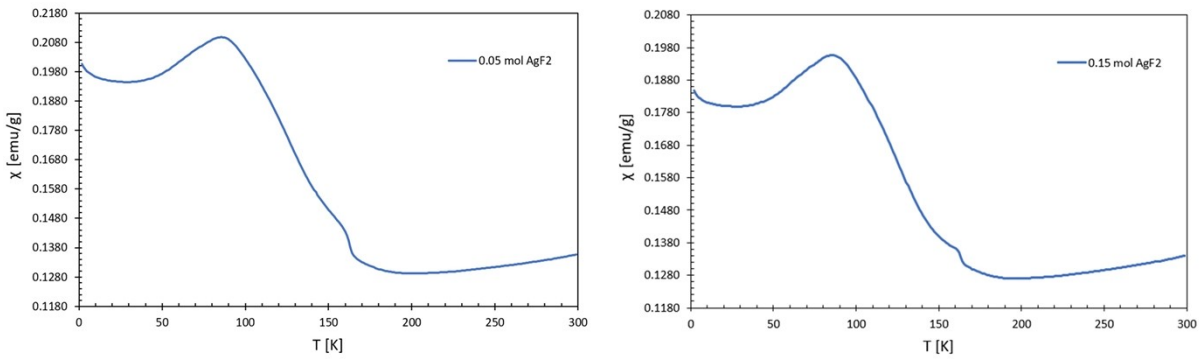

Figure SI7. Magnetic susceptibility at 10k Oe of sample 1 (**S1**) after subtracting the contribution of

0.05 mol% (left) and 0.15 mol% (right) of AgF_2 to overall magnetic response.

SI.VI Results of superexchange calculations

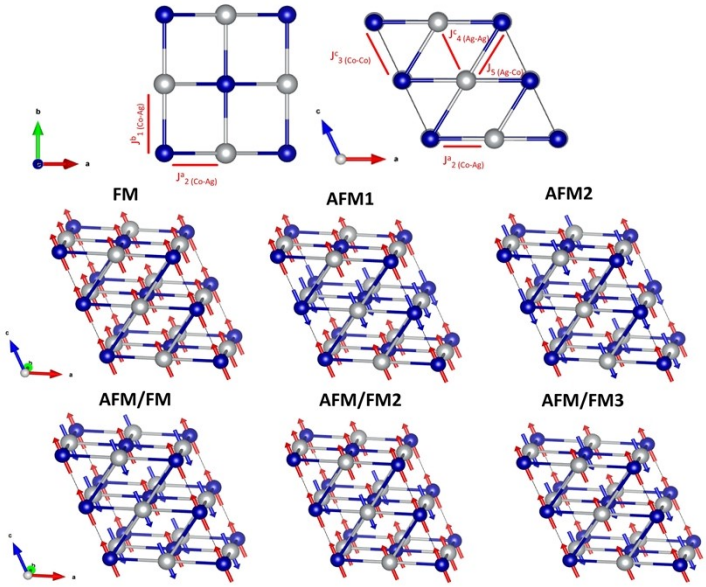

Figure SI8. Superexchange paths (top) and six possible spin states for $AgCoF_5$. The fluorine atoms have been omitted for clarity. Blue and red arrows indicate opposite spin directions. AFM2 is the spin state with the lowest energy.

Table SI8. Superexchange constants determined with the DFT+U, SCAN and HSE06 methods.

Method	$J^b_{1(Co\text{-}Ag)}$ [010] [meV]	$J^a_{2(Co\text{-}Ag)}$ [100] [meV]	$J^c_{3(Co\text{-}Co)}$ [001] [meV]	$J^c_{4(Ag\text{-}Ag)}$ [001] [meV]	$J_{5(Ag\text{-}Co)}$ [101] [meV]	Magnetic moments [μ_B] Ag	Co
DFT+U (U_{Ag}=5 eV)	-47.74	-6.53	-8.28	-1.11	-1.23	+/-3.22	+/-0.58
DFT+U (U_{Ag}=8 eV)	-39.25	-6.52	-8.21	-0.37	-1.36	+/-3.24	+/-0.66
SCAN	-62.02	-4.77	-10.28	-1.34	-1.91	+/-3.09	+/-0.54
HSE06	-39.49	-6.74	-7.96	0.70	-0.52	+/-3.47	+/-0.73

SI.VII References

[1] A. Tressaud, J. M. Dance, J. Ravez, J. Portier, P. Hagenmuller, J. B. Goodenough, *Materials Research Bulletin* **1973**, *8*, 1467–1477.

[2] G. Ferey, R. Pape, *Acta Cryst.* **1978**, 1084–1091.

[3] U. Müller, R. Hoppe, *Z. Anorg. Allg. Chem.* **1990**, *583*, 205–208.

[4] J. Graulich, W. Massa, D. Babel, *Z. anorg. allg. Chem.* **2003**, *629*, 365–367.

[5] K. K. Wu, I. D. Brown, *Materials Research Bulletin* **1973**, *8*, 593–598.

[6] S. M. Eicher, J. E. Greedan, *Journal of Solid State Chemistry* **1984**, *52*, 12–21.

[7] R. Von Der Mühll, S. Andersson, J. Galy, *Acta Crystallogr B Struct Crystallogr Cryst Chem* **1971**, *27*, 2345–2353.

[8] R. Georges, J. Ravez, R. Olazcuaga, P. Hagenmuller, *Journal of Solid State Chemistry* **1974**, *9*, 1–5.

[9] R. von der Mühll, F. Daut, J. Ravez, *Journal of Solid State Chemistry France* **1973**, *8*, 206–212.

[10] A. Tressaud, J. M. Parenteau, J. M. Dance, J. Portier, P. Hagenmuller, **1973**, *8*.

[11] M. Body, G. Silly, C. Legein, J.-Y. Buzaré, F. Calvayrac, P. Blaha, *Journal of Solid State Chemistry* **2005**, *178*, 3655–3661.

[12] J. Ravez, M. Darriet, R. Von der Mühll, P. Hagenmuller, *Journal of Solid State Chemistry* **1971**, *3*, 234–237.

[13] J. Grannec, J. Ravez, *C. R. Acad. Sc. Série C* **1970**, *270*, 2059–2061.